

# Appendix A

## A Search for Sub-millisecond Pulsations from Unidentified FIRST and NVSS Radio Sources

This chapter is a modified self-contained paper titled, “A Search for Sub-millisecond Pulsations from Unidentified FIRST and NVSS Radio Sources,” which has been published in the *Astronomical Journal* (Crawford, Kaspi, & Bell 2000).

We have searched 92 unidentified sources from the FIRST and NVSS 1400-MHz radio survey catalogs for radio pulsations at 610 MHz. The selected radio sources are bright, have no identification with extragalactic objects, are point-like and are more than 5% linearly polarized. Our search was sensitive to sub-millisecond pulsations from pulsars with dispersion measures (DMs) less than  $\sim 500 \text{ pc cm}^{-3}$  in the absence of scattering. We have detected no pulsations from these sources and consider possible effects which might prevent detection. We conclude that as a population, these sources are unlikely to be pulsars.

### A.1 Introduction

The FIRST survey (Faint Images of the Radio Sky at Twenty Centimeters) and NVSS survey (NRAO VLA Sky Survey) are recent 1400-MHz VLA radio surveys of

the Northern sky. The FIRST survey is an ongoing survey of the North and South Galactic caps using the VLA in B-configuration with a synthesized beam size of  $5.4''$  (Becker, White, & Helfand 1995). In the published FIRST catalog of radio sources from the first two observing sessions in 1993 and 1994 (White et al. 1997), 1550 square degrees of the North Galactic cap were covered spanning  $7^{\text{h}} < \alpha(\text{J2000}) < 18^{\text{h}}$  and  $+28^\circ < \delta(\text{J2000}) < +42^\circ$ . The positions and flux densities of  $\sim 1.4 \times 10^5$  discrete radio sources<sup>1</sup> are complete down to a flux density of  $\sim 1$  mJy. The NVSS survey (Condon et al. 1998) covers  $\delta > -40^\circ$  (covering 82% of the celestial sphere) and catalogs more than  $1.8 \times 10^6$  sources complete down to a flux density of  $\sim 2.5$  mJy. The NVSS survey was conducted with the VLA in D and DnC configurations with a synthesized beam size of  $45''$ . The NVSS survey also preserves polarization information.

Several large-scale pulsar surveys have previously been conducted at high Galactic latitudes (see Camilo 1997 and references therein). However, the rates at which the received analog power was sampled and digitized in these surveys, typically 3-4 kHz, and the low observing radio frequencies ( $\sim 400$  MHz), combined with relatively large radio frequency channel bandwidths of between 125 kHz and 1 MHz, restricted their sensitivity to sub-millisecond pulsars to very small dispersion measures (DMs) ( $\text{DM} \lesssim 10 \text{ pc cm}^{-3}$ ). Large-scale surveys that maintain sensitivity to sub-millisecond periodicities over a wide range of DMs are difficult: the fast sampling rate and small radio frequency channel bandwidth required make large total bandwidths and long integration times currently impractical. However, a targeted search for sub-millisecond pulsations is possible using narrow frequency channels and a fast sampling rate. Such a survey is of course also sensitive to long-period pulsars which may have been missed in previous surveys due to radio frequency interference (RFI) or scintillation.

Consideration of the properties of known recycled pulsars and representative models of magnetic field decay and equations of state suggests that a significant population of sub-millisecond pulsars could be present in the Galaxy (e.g., Possenti et al.

---

<sup>1</sup>The online catalog is updated regularly as observing proceeds and currently contains more than  $5.4 \times 10^5$  sources derived from data taken from 1993 to 1998 (99Jul21 catalog version, <http://sundog.stsci.edu/first/catalogs.html>).

1998). It is possible, therefore, that some of the sources which remain unidentified in radio survey catalogs could be bright sub-millisecond radio pulsars which have previously escaped detection in high-latitude pulsar surveys. To date, no pulsar has been found with a period shorter than that of the first millisecond pulsar discovered, PSR J1939+2134 (B1937+21), which has a 1.56-ms period (Backer et al. 1982). The discovery of a sub-millisecond pulsar would place important constraints on the equation of state of neutron star matter at high densities (e.g., Kulkarni 1992).

## A.2 Target Choice and Observations

The FIRST and NVSS surveys contain a number of bright sources which are unresolved and have no identification in other wavebands. Although over 99% of bright sources ( $S_{1400} > 60$  mJy) found in previous large-scale surveys are believed to be active galactic nuclei (AGN) (Condon et al. 1998), many sources in the FIRST and NVSS catalogs remain unidentified. One possibility is that they are previously unrecognized radio pulsars. Since pulsars often have a high degree of linear polarization (Lyne & Manchester 1988), polarized sources are good targets for pulsar searches. Han & Tian (1999) have identified 97 objects in the NVSS catalog which are coincident with known pulsars. Of the 89 redetected pulsars in Table 1 of their paper for which the degree of linear polarization could be determined from the NVSS observations, only 8 had an observed nominal fractional linear polarization less than 5%. The intrinsic degree of polarization of these pulsars may even be higher if bandwidth depolarization effects are significant, in which case an even higher fraction of the pulsar sample is more than 5% linearly polarized. Figure 2 of Han & Tian (1999) shows that only  $\sim 10\%$  of identified quasars and  $\sim 10\%$  of BL-Lac objects are more than 5% linearly polarized. Thus, although there is not a clear polarization cutoff separating the pulsar and extragalactic populations, a polarization threshold of 5% excludes most ( $\sim 90\%$ ) of the identified non-pulsar population while retaining the majority ( $\sim 90\%$ ) of the identified pulsar population.

We have searched for radio pulsations in bright ( $S_{1400} \geq 15$  mJy) point-like uniden-

tified sources from the FIRST and NVSS survey catalogs which are more than 5% linearly polarized at 1400 MHz. Sources were selected directly from the catalogs if they met certain criteria.

Unidentified FIRST sources had their flux densities checked against their corresponding NVSS flux densities. If a source was extended, the better resolution of the FIRST survey would be expected to yield a lower flux density for the source than the NVSS survey. Therefore, in order to eliminate extended objects, sources were only included if their FIRST and NVSS flux densities agreed to within a few percent (indicating an unresolved non-variable source) or if the FIRST flux density exceeded the NVSS flux density (indicating an unresolved scintillating source). The large number of extended sources in the catalogs makes this filter necessary, though it does unfortunately eliminate scintillating sources which happen to be fainter in the FIRST survey.

For unresolved NVSS sources outside of the FIRST survey region, pointed VLA observations were undertaken in October 1995 in B-configuration in order to obtain the same angular resolution ( $5.4''$ ) as the FIRST survey (R. Becker & D. Helfand, unpublished work). Sources in these observations were then subjected to the selection criteria described above. A total of 92 objects from the catalogs (39 appearing in both FIRST and NVSS, and 53 appearing only in NVSS) fit our selection criteria and were sufficiently far north to be observed in our search. The positions, NVSS total intensity peak flux densities, and fractional linear polarization from the NVSS peak flux density values are listed for the selected sources in Tables A-1 and A-2.

Each of the 92 unidentified sources was observed at a center frequency of 610 MHz in two orthogonal linear polarizations for 420 s with the Lovell 76-meter telescope at Jodrell Bank, UK. A total bandwidth of 1 MHz was split into 32 frequency channels with detected signals from each channel added in polarization pairs and recorded on Exabyte tape as a continuous one-bit digitized time series sampled at  $50 \mu\text{s}$ . The minimum detectable flux density of periodicities in a pulsar search depends upon the raw sensitivity of the system and a number of propagation and instrumental effects (Chapter 2; see also, e.g., Dewey et al. 1985). Interstellar dispersion contributes to

Table A-1. Positions of Observed FIRST/NVSS Sources

Source	$\alpha$ (J2000) (hh:mm:ss.sss)	$\delta$ (J2000) (dd:mm:ss.ss)	Source	$\alpha$ (J2000) (hh:mm:ss.sss)	$\delta$ (J2000) (dd:mm:ss.ss)
0002-1952	00:02:40.965	-19:52:52.43	0755+3013	07:55:01.887	+30:13:46.68
0004-1148	00:04:04.905	-11:48:58.52	0755+3341	07:55:36.599	+33:41:56.27
0011-2254	00:11:09.912	-22:54:58.64	0757+2721	07:57:52.648	+27:21:07.62
0014-2800	00:14:44.065	-28:00:47.39	0758+3929	07:58:08.846	+39:29:28.61
0023-2155	00:23:30.215	-21:55:37.73	0802+3122	08:02:12.783	+31:22:40.56
0024+0308	00:24:49.369	+03:08:34.65	0805+2737	08:05:19.023	+27:37:35.99
0026-1112	00:26:51.454	-11:12:52.57	0806+3310	08:06:01.704	+33:10:10.16
0027-3030	00:27:02.074	-30:30:32.16	0810+3034	08:10:40.249	+30:34:32.99
0032-2649	00:32:33.032	-26:49:17.70	0840+2923	08:40:30.750	+29:23:32.57
0037-2323	00:37:08.808	-23:23:40.65	0843+3738	08:43:08.663	+37:38:16.42
0040+1329	00:40:21.805	+13:29:37.72	0844+3629	08:44:56.087	+36:29:27.64
0051+0229	00:51:51.304	+02:29:44.11	0846+3746	08:46:47.432	+37:46:14.97
0054-1754	00:54:10.786	-17:54:13.32	0903+3523	09:03:05.211	+35:23:18.91
0057+1341	00:57:36.448	+13:41:45.24	0911+3349	09:11:47.745	+33:49:16.60
0107-1211	01:07:11.786	-12:11:23.96	0923+3011	09:23:30.450	+30:11:10.92
0114-3219	01:14:48.887	-32:19:51.76	0928+4142	09:28:22.186	+41:42:21.77
0138-2954	01:38:40.505	-29:54:46.04	0944+3803	09:44:59.202	+38:03:17.34
0146+0222	01:46:14.619	+02:22:08.16	1000+3718	10:00:21.815	+37:18:44.99
0147+0715	01:47:27.777	+07:15:02.82	1003+3244	10:03:57.560	+32:44:02.87
0154-2422	01:54:56.898	-24:22:33.61	1013+3445	10:13:49.574	+34:45:50.74
0214+1027	02:14:59.232	+10:27:48.65	1033+2851	10:33:19.483	+28:51:22.16
0217-2354	02:17:50.767	-23:54:56.42	1126+3418	11:26:12.536	+34:18:20.67
0223+0732	02:23:33.975	+07:32:18.99	1129+3622	11:29:51.387	+36:22:15.70
0223+1159	02:23:40.829	+11:59:10.11	1145+3145	11:45:23.236	+31:45:17.24
0224+1357	02:24:41.842	+13:57:33.00	1146+2601	11:46:08.554	+26:01:05.58
0238-3032	02:38:55.197	-30:32:02.67	1150+3020	11:50:43.890	+30:20:17.66
0249+1237	02:49:44.482	+12:37:06.27	1201+2550	12:01:25.648	+25:50:04.55
0251-1742	02:51:06.234	-17:42:39.77	1201+3129	12:01:44.264	+31:29:03.22
0258-3146	02:58:05.951	-31:46:27.90	1220+3111	12:20:04.656	+31:11:45.04
0259+0747	02:59:27.067	+07:47:39.06	1234+2917	12:34:54.323	+29:17:43.93
0259+4708	02:59:04.207	+47:08:40.31	1236+3706	12:36:50.831	+37:06:02.01
0317+0606	03:17:26.849	+06:06:14.53	1242+2721	12:42:19.687	+27:21:57.32
0322-3458	03:22:13.098	-34:58:33.34	1251+3643	12:51:24.132	+36:43:57.27
0326-3243	03:26:15.123	-32:43:24.41	1334+3434	13:34:26.833	+34:34:25.11
0349+0354	03:49:14.315	+03:54:45.34	1343+2903	13:43:24.006	+29:03:57.55
0403+6445	04:03:42.805	+64:45:56.01	1414+4022	14:14:40.585	+40:22:25.75
0421+3511	04:21:19.710	+35:11:15.79	1426+4035	14:26:58.101	+40:35:38.36
0458+4953	04:58:28.750	+49:53:55.67	1434+3805	14:34:46.988	+38:05:14.87
0505+2606	05:05:54.171	+26:06:25.03	1458+3720	14:58:44.704	+37:20:22.15
0518+6439	05:18:43.662	+64:39:57.72	1508+2818	15:08:08.312	+28:18:13.51
0606+4401	06:06:50.206	+44:01:40.73	1547+3954	15:47:40.147	+39:54:38.48
0607+2915	06:07:18.949	+29:15:27.64	1606+2709	16:06:16.249	+27:09:28.69
0620+7334	06:20:52.108	+73:34:41.12	1609+2628	16:09:50.978	+26:28:38.72
0701+2631	07:01:20.742	+26:31:56.95	1618+2931	16:18:27.685	+29:31:17.99
0719+2935	07:19:22.188	+29:35:43.30	1635+3751	16:35:53.071	+37:51:54.59
0733+3331	07:33:13.289	+33:31:51.81	2321-1758	23:21:02.411	-17:58:22.09

Table A-2. Parameters of Observed FIRST/NVSS Sources

Source	FIRST Source?	$S_{1400}^a$ (mJy)	% poln <sup>b</sup>	Source	FIRST Source?	$S_{1400}^a$ (mJy)	% poln <sup>b</sup>
0002-1952	N	58	9	0755+3013	Y	51	11
0004-1148	N	450	6	0755+3341	Y	81	7
0011-2254	N	37	9	0757+2721	Y	44	7
0014-2800	N	52	14	0758+3929	N	530	8
0023-2155	N	135	8	0802+3122	N	84	10
0024+0308	N	68	9	0805+2737	N	41	9
0026-1112	N	166	7	0806+3310	N	44	6
0027-3030	N	24	13	0810+3034	Y	152	6
0032-2649	N	131	6	0840+2923	Y	17	13
0037-2323	N	66	5	0843+3738	Y	108	11
0040+1329	N	34	9	0844+3629	Y	49	6
0051+0229	N	15	20	0846+3746	N	21	15
0054-1754	N	29	11	0903+3523	Y	57	6
0057+1341	N	64	8	0911+3349	Y	370	7
0107-1211	N	56	6	0923+3011	Y	34	6
0114-3219	N	122	16	0928+4142	N	96	12
0138-2954	N	45	10	0944+3803	N	42	11
0146+0222	N	136	8	1000+3718	Y	35	9
0147+0715	N	237	6	1003+3244	Y	419	7
0154-2422	N	45	10	1013+3445	Y	350	6
0214+1027	N	27	12	1033+2851	Y	29	9
0217-2354	N	82	11	1126+3418	Y	39	7
0223+0732	N	128	12	1129+3622	Y	119	6
0223+1159	N	34	9	1145+3145	Y	77	10
0224+1357	N	93	9	1146+2601	Y	114	7
0238-3032	N	155	5	1150+3020	Y	31	13
0249+1237	N	255	6	1201+2550	Y	20	24
0251-1742	N	65	12	1201+3129	Y	87	6
0258-3146	N	242	8	1220+3111	Y	28	8
0259+0747	N	807	5	1234+2917	Y	434	9
0259+4708	N	107	9	1236+3706	Y	62	9
0317+0606	N	196	8	1242+2721	Y	69	10
0322-3458	N	49	7	1251+3643	Y	29	8
0326-3243	N	93	5	1334+3434	Y	48	7
0349+0354	N	147	8	1343+2903	Y	22	17
0403+6445	N	72	5	1414+4022	Y	43	6
0421+3511	N	68	9	1426+4035	Y	28	9
0458+4953	N	19	12	1434+3805	Y	149	9
0505+2606	N	23	9	1458+3720	Y	210	6
0518+6439	N	28	12	1508+2818	Y	76	7
0606+4401	N	145	8	1547+3954	Y	128	15
0607+2915	N	25	14	1606+2709	Y	29	7
0620+7334	N	84	9	1609+2628	Y	17	15
0701+2631	N	32	11	1618+2931	Y	29	8
0719+2935	Y	15	14	1635+3751	Y	47	6
0733+3331	N	19	13	2321-1758	N	17	13

<sup>a</sup>NVSS catalog total intensity 1400-MHz peak flux density.

<sup>b</sup>NVSS catalog percent linear polarization from 1400-MHz peak flux densities.

the broadening of the intrinsic pulse according to

$$\tau_{\text{DM}} = \left(\frac{202}{\nu}\right)^3 \text{DM} \Delta\nu. \quad (\text{A.1})$$

Here  $\tau_{\text{DM}}$  is in milliseconds,  $\nu$  is the observing frequency in MHz, DM is the dispersion measure in  $\text{pc cm}^{-3}$ , and  $\Delta\nu$  is the channel bandwidth in MHz. For our observing system,  $\tau_{\text{DM}}$  is  $1.135 \mu\text{s}$  per  $\text{pc cm}^{-3}$  of DM. The fast sampling rate ( $t_{\text{samp}} = 50 \mu\text{s}$ ) and small channel bandwidth ( $\Delta\nu = 31.25 \text{ kHz}$ ) in our survey made it sensitive to sub-millisecond pulsars for a large range of DMs ( $\text{DM} \lesssim 500 \text{ pc cm}^{-3}$ ) in the absence of pulse scattering effects. Our estimated sensitivity to pulsations for a range of periods and DMs is shown in Figure A-1. The method used to produce Figure A-1 follows the one described in Chapter 2 for the Parkes Multibeam Pulsar Survey.

### A.3 Data Reduction

In each observation, the frequency channels were dedispersed at 91 trial DMs which ranged from 0 to  $1400 \text{ pc cm}^{-3}$  and were summed. We searched this large DM range in the unlikely event that a source could be a previously missed long-period pulsar with a high DM. For  $\text{DM} \gtrsim 500 \text{ pc cm}^{-3}$  the channel dispersion smearing is too great to maintain sensitivity to sub-millisecond pulsations from all our sources. However, the Taylor & Cordes (1993) model of the Galactic free electron distribution indicates that for all of our sources, with the exception of two that are within  $5^\circ$  of the Galactic plane, the DMs are expected to be less than  $100 \text{ pc cm}^{-3}$  regardless of distance. Each resulting dedispersed time series of  $2^{23}$  samples was then coherently Fourier transformed to produce an amplitude modulation spectrum corresponding to a trial DM.

RFI produced many false peaks in certain narrow regions of the modulation spectra at low DMs. We therefore masked several frequency ranges and their harmonics in which RFI appeared regularly so that any true pulsar signals were not swamped by interference. Typically 1-2% of the modulation spectrum in each observation was lost in this way.

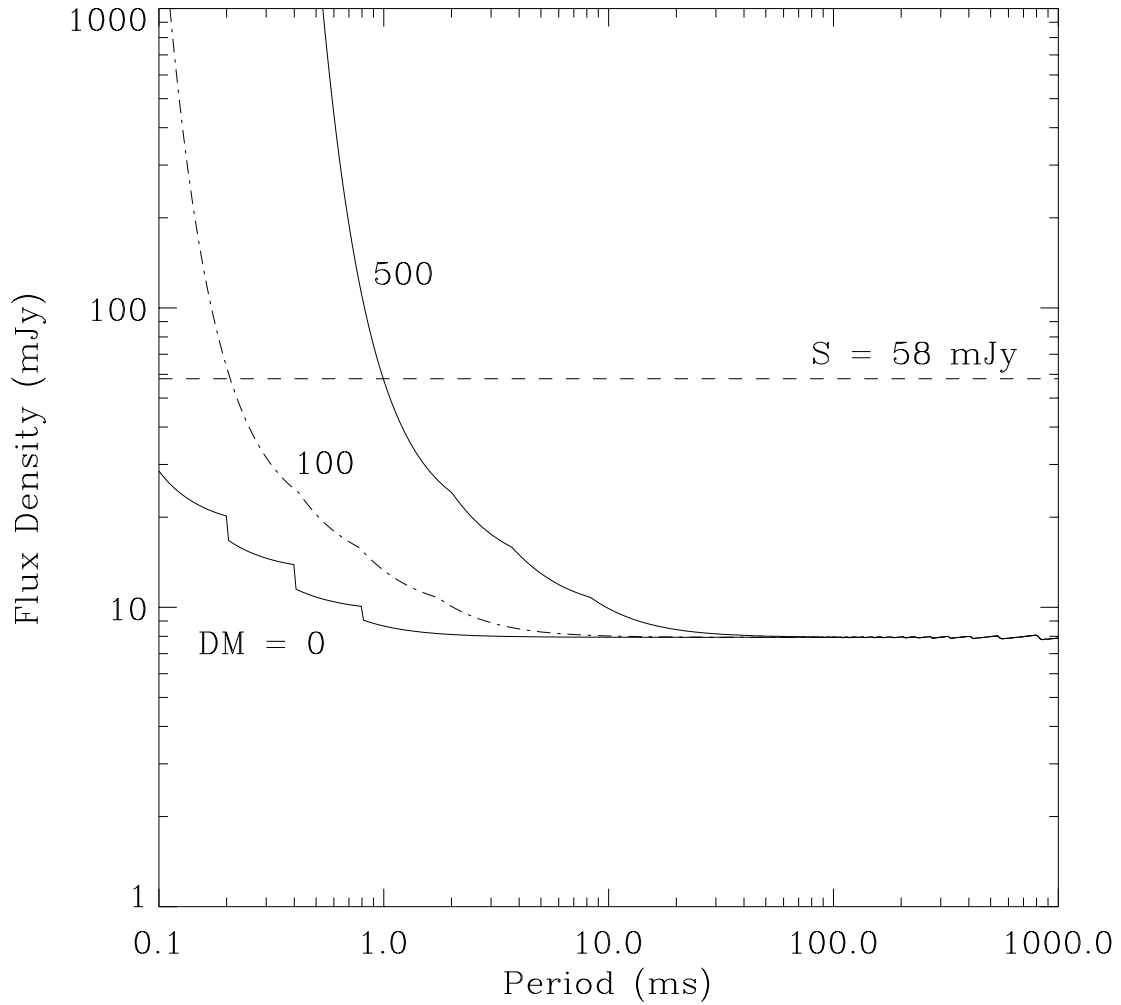


Figure A-1 Pulsar sensitivity curves for DMs of 0, 100, and 500  $\text{pc cm}^{-3}$ , assuming a 5% intrinsic pulsed duty cycle. The dashed horizontal line at 58 mJy is the flux density of our weakest source at 600 MHz, assuming a typical pulsar spectral index of  $\alpha = -1.6$ . All of our sources are expected to have  $\text{DM} < 100 \text{ pc cm}^{-3}$  (indicated by the dashed-dotted line).

We then looked for the strongest peaks in the spectra. First, each modulation spectrum was harmonically summed. In this process, integer harmonics in the modulation spectrum are summed, enhancing sensitivity to harmonic signals (e.g., Nice, Fruchter, & Taylor 1995). This is particularly useful for long-period pulsars, which have a large number of unaliased harmonics. After summing up to 16 harmonic signals, the highest candidate peaks in the modulation spectrum were recorded along with the period, DM, and the signal-to-noise ratio (S/N). Redundant harmonic candidates were then eliminated. Unique candidates were recorded if they had  $S/N > 7$  and if the candidate period appeared in at least 10 DM trials. The final candidates for each beam were inspected by dedispersing the original data at DMs near the candidate DM and folding the data at periods near the candidate period in order to look for a broad-band, continuous pulsar-like signal.

This technique was tested by observing several known bright pulsars, PSR J1939+2134, PSR J0332+5434 (B0329+54), and PSR J2145–0750, throughout the survey. The results for these pulsars are listed in Table A-3. All three pulsars were detected with S/N consistent with our survey sensitivity, though scintillation affects the detection strengths.

## A.4 Discussion

We did not detect any significant pulsations from the target sources. Here we consider possible effects which could prevent detection if they were pulsars.

### A.4.1 Source Brightness

The selected sources were bright, with the weakest source having a 1400-MHz flux density of 15 mJy. Assuming a typical pulsar spectral index of  $\alpha = -1.6$  (Lorimer et al. 1995), where  $\alpha$  is defined according to  $S \sim \nu^\alpha$ , this source would have flux density 58 mJy at 600 MHz (the horizontal dashed line in Figure A-1). For expected DMs, this is about seven (four) times greater than our sensitivity limit for periods greater than (about equal to) 1 ms, as indicated in Figure A-1. All of our sources, therefore,

were bright enough (in the absence of scintillation) to be easily detectable with our observing system if they were pulsars.

### **A.4.2 Dispersion Smearing and Scattering**

Dispersion smearing is not a factor preventing detection, since all but two of these sources have high Galactic latitudes ( $|b| > 5^\circ$ ) and should have  $DM < 100 \text{ pc cm}^{-3}$  regardless of distance. This is well within our sensitivity limits to sub-millisecond pulsations (see Figure A-1). Interstellar scattering, which can be estimated from the Taylor & Cordes (1993) model of the Galactic electron distribution, is expected to be negligible at 610 MHz. Two of the sources (0458+4953 and 0607+2915) are within  $5^\circ$  of the Galactic plane; for an assumed DM of  $100 \text{ pc cm}^{-3}$ , their predicted pulse scatter-broadening times are  $\sim 140 \mu\text{s}$  at 610 MHz. This is small enough to maintain sensitivity to sub-millisecond pulsations, and is of the same order as the dispersion smearing ( $113 \mu\text{s}$ ) at this DM.

### **A.4.3 Wide Beaming**

An extremely wide beam would prevent modulation of the pulsed signal and could render a pulsar undetectable. However, this would likely occur only in an aligned rotator geometry in which both the spin and magnetic axes are pointing toward us. This is unlikely for our targets, since, if they were pulsars, the position angle of linear polarization is expected to follow the projected direction of the magnetic axis as the star rotates (Lyne & Manchester 1988). This geometry would significantly reduce the measured degree of linear polarization as the pulsar rotates, inconsistent with our choice of significantly polarized sources.

### **A.4.4 Scintillation**

Scintillation is the modulation of a radio signal passing through a medium of variable index of refraction, such as an inhomogeneous interstellar plasma. In diffraction scintillation, the wave scattering causes interference which can enhance or suppress

the amplitude of the radio signal on the time scale of minutes (e.g., Manchester & Taylor 1977). These intensity fluctuations vary as a function of radio frequency at any given time and have a characteristic bandwidth  $\Delta\nu$ , where

$$\Delta\nu \simeq 11 \nu^{22/5} d^{-11/5}. \quad (\text{A.2})$$

Here  $\Delta\nu$  is in MHz,  $\nu$  is the observing frequency in GHz, and  $d$  is the distance to the source in kpc (Cordes, Weisberg, & Boriakoff 1985). For pulsars with  $d < 1$  kpc, this characteristic bandwidth exceeds our 610 MHz observing bandwidth of 1 MHz. Indeed, of 28 nearby pulsars observed at 660 MHz by Johnston, Nicastro, & Koribalski (1998), 13 had scintillation bandwidths greater than our bandwidth of 1 MHz and had a characteristic fluctuation time-scale greater than our integration time of 420 s. More than half of these 13 pulsars had distances less than 1 kpc, and only one had  $d > 2$  kpc. If the sources we surveyed were placed at a distance of 2 kpc and a spectral power law index of  $\alpha = -1.6$  is assumed, their 400-MHz luminosities would all be at the upper end of the observed pulsar luminosity distribution ( $L_{400} > 450 \text{ mJy kpc}^2$ ). This suggests that if these sources were pulsars, they are likely to be closer than 2 kpc and therefore in the distance range where the scintillation bandwidth exceeds our observing bandwidth. In this case, scintillation causes the probability distribution of the observed intensity to be an exponential function with a maximum in the distribution at zero intensity (McLaughlin et al. 1999). The number of sources we expect to see in our sample is the sum of the probabilities that we will see each individual source (i.e., that the scintillated flux is above the minimum detectable flux). For the range  $P > 1$  ms, we expect to see 88 of the 92 sources (5% missed). For the range  $P \sim 1$  ms, we expect to see 85 of the 92 sources (8% missed). Thus, only a few of our sources are likely to have been missed due to scintillation. Therefore scintillation cannot account for the non-detection of the bulk of the sources in the survey.

### A.4.5 Binary Orbital Motion

A pulsar in a binary orbit experiences an acceleration which changes the observed modulation frequency during the course of the observation. Sensitivity to pulsations is degraded if the frequency drift exceeds a single Fourier bin  $\Delta f = 1/T_{\text{int}}$ , where  $T_{\text{int}}$  is the integration time. Assuming that the acceleration of the pulsar is constant during the observation, a critical acceleration can be defined, above which the change in frequency is greater than  $\Delta f$  and the sensitivity is reduced:

$$a_{\text{crit}} = \frac{c}{fT_{\text{int}}^2}. \quad (\text{A.3})$$

Since the Fourier drift scales linearly with acceleration, the reduction in sensitivity scales linearly with acceleration. For our integration time of 420 s, the critical acceleration is  $a_{\text{crit}}/P \sim 1.7$  (where  $a_{\text{crit}}$  is in units of  $\text{m s}^{-2}$  and  $P$  is the pulsar period in ms). Our weakest source is several times brighter than our detection limit (Figure A-1), so a reduction in sensitivity by a factor of several should still maintain detectability to pulsations. Thus, a more appropriate critical acceleration for the weakest source in our list is  $a_{\text{crit}}/P \sim 12$  (for  $P > 1$  ms) and  $a_{\text{crit}}/P \sim 7$  (for  $P \sim 1$  ms).

Orbits containing millisecond or sub-millisecond pulsars that have been spun up from mass transfer from a low-mass donor would be expected to be circular. Of the 40 known pulsars in circular ( $e < 0.01$ ) binary orbits, the largest projected mean acceleration to our line of sight (assuming  $i = 60^\circ$ ) is  $a_{\text{mean}}/P \sim 3.6$  for PSR J1808–3658, an X-ray millisecond pulsar with a 2.5-ms period in a 2-h binary orbit around a  $0.05 M_\odot$  companion (Chakrabarty & Morgan 1998). This acceleration is well below the critical acceleration  $a_{\text{crit}}/P$  even for our weakest source.

The mean flux density of the sources on our list, however, is much higher ( $S_{610} \sim 400$  mJy, assuming  $\alpha = -1.6$ ) than our weakest source, which raises the critical acceleration for our typical source. Only very large accelerations ( $a_{\text{mean}}/P \gtrsim 85$  for  $P > 1$  ms and  $a_{\text{mean}}/P \gtrsim 40$  for  $P \lesssim 1$  ms) would prevent detection of pulsations for our typical source. A system such as PSR J1808–3658 with  $S_{610} \sim 400$  mJy would still be detectable if it had  $P \sim 0.3$  ms or if it had an orbital period  $P_b \sim 15$

minutes (but not both). Thus it is unlikely that binary motion in a sub-millisecond or millisecond pulsar system would be a significant source of non-detections for most of our sources.

#### **A.4.6 Likelihood of Serendipitous Detection**

We have also estimated the likelihood of serendipitously detecting a pulsar not associated with these sources using the observed surface density of both normal and millisecond pulsars in the Galactic plane (Lyne et al. 1998). With standard assumptions for a spectral power law index and luminosity distribution (Lorimer et al. 1993), we find that it is unlikely ( $< 2\%$  probability) that we would detect any pulsars from the chance placement of our 92 beams.

### **A.5 Conclusions**

No pulsations were detected at 610 MHz from the 92 polarized, point-like sources that we searched from the FIRST and NVSS radio surveys. Sensitivity to sub-millisecond pulsations was maintained for DMs less than about  $500 \text{ pc cm}^{-3}$  (in the absence of scattering effects), which encompasses the expected DM range for all of these sources. We find that several effects which could prevent detection (brightness, dispersion smearing, scattering, and beaming) are not significant factors here. Scintillation is expected to account for only a few of our non-detections and therefore cannot be the cause of the majority of our non-detections. For a source with a typical flux density in our list, Doppler motion in a tight binary system would only prevent detection if the mean projected line-of-sight acceleration of the pulsar were at least an order of magnitude higher than those observed in the known population of circular binary pulsar systems. We conclude that as a population, these sources are unlikely to be pulsars. Given that  $\sim 10\%$  of extragalactic sources in the NVSS survey were identified by Han & Tian (1999) as being at least 5% linearly polarized, it is possible that most of our target sources are unidentified extragalactic objects. However, the nature of these sources is still not certain.

Table A-3. Observed Test Pulsars

PSR	$P$ (ms)	DM (pc cm <sup>-3</sup> )	$S_{1400}$ <sup>a</sup> (mJy)	$S_{600}$ <sup>b</sup> (mJy)	S/N
J0332+5434	714.52	26.8	203	785	725
J1939+2134	1.56	71.0	16	100	46
J2145-0750	16.05	9.0	10	30	36

<sup>a</sup>Catalog 1400-MHz flux density (Taylor, Manchester, & Lyne 1993).

<sup>b</sup>Catalog 600-MHz flux density (Taylor, Manchester, & Lyne 1993).